COBEM 2023 27TH INTERNATIONAL CONGRESS OF MECHANICAL ENGINEERING

ABCM Brazilian Society of Mechanical Sciences and Engineering
27th ABCM International Congress of Mechanical Engineering
December 04-08, 2023, Florianópolis-SC, Brazil

COB-2023-2194
DESIGN OPTIMIZATION OF SOURCES IN FLUID FLOW SYSTEMS USING COMPUTATIONAL FLUID DYNAMICS-BASED ADJOINT METHOD

Javier Aliaga Rivera [1]
Marcos Sebastião de Paula Gomes [2]
[1,2]Pontifícia Universidade Católica do Rio de Janeiro - Departamento de Engenharia Mecânica
Av. Marquês de São Vicente 225, CEP22453-900, Rio de Janeiro, RJ, Brazil.
[1]javieraliaga2009@yahoo.es
[2] mspgomes@puc-rio.br

Abstract. *In this study, we develop a method for design optimization of a discrete number of sources in fluid flow systems using computational fluid dynamics-based adjoint method. The optimal location and magnitude of discrete sources in the domain, to achieve a determined steady-state condition, is the focus of our research. To this end, we present the derivation of the sensitivities with respect to the coordinates and magnitude of the sources, using the continuous adjoint method. The comparison of the calculated sensitivities with the ones obtained from the Finite Difference Method proves the accuracy and robustness of the proposed method, allowing the systematic evaluation of such sensitivities without the need to resort to automatic differentiation or the expense associated with finite difference approximations. The principal motivation for this work comes from problems in optimal design of valves and flow control. To illustrate the method, standard scalar transport in steady-state is first presented in one dimension, followed by an extension to two dimensions. Furthermore, a number of numerical studies are carried out for different configurations and operating conditions. The different cases demonstrate the method's capability by applying it to the optimal design of location and magnitude of distributed sources with little computational effort. Finally, possible applications and limitations of the methodology are discussed.*

Keywords: *Continuous adjoint, source optimization, parametric optimization, CFD.*

1. INTRODUCTION

Currently the CFD-based Adjoint method remains as a suitable approach for optimization in fluid dynamics. Depending on the type of design variables, the Adjoint method is used predominantly in shape (Soto *et al.*, 2004), topology (Othmer, 2008), flow control (Rimer, 2016) and parametric (Kouhi *et al.*, 2016) optimization problems.

In parametric optimization, the system is described through some parameters that can be related to the geometry, physical properties, magnitude and location of sources and inlets, among others. The value of this parameters varies until a configuration considered optimized is reached. Particular studies of interest are related to thermal and mass transfer to create desired enclosed environments by inverse design method as shown by Liu (2017) and Nabi *et al.* (2017). Kouhi *et al.* (2016) presented a framework based on the discrete adjoint method for evaluating the sensitivities of a set of parameters related to chemically reacting flows.

The optimal location, strength, size and shape of sources, which basically have its application in thermal comfort and indoor air-quality, represents a design problem that requires additional working out. Eriksson (2017) performed a thermal design optimization in a unit square domain with parameterized source terms corresponding to components heated by resistive heating. Nevertheless, the maximum number of sources was only three, and the sensitivity analysis was computed by finite difference method.

In this work we aim to optimize the location of sources that follows the Brinkman penalization approach, in order to represent solid regions. Inspired in the Immersed boundary method (Boffi *et al.*, 2005), we discretize the governing equations in an Eulerian grid on the fluid and the sources in a separate Lagrangian framework through interpolation methods. The determination of the sensitivity of an arbitrary objective function in relation to the position of sources, whether they are dependent or independent of the state variables, is a novel contribution from this work. Examples are first presented in one dimension for a scalar transport equation, followed by an extension to two dimensions of the Navier-stokes equation in steady-state and laminar regime. The issue with the continuous adjoint method is the proper implementation of the adjoint boundary conditions and the method of solution. The implementation of boundary conditions by FEM and FVM are fairly different. The adjoint equation is linear, so it can be solved either by a direct method with the FEM, i.e. $Ax = B$ where $x = A^{-1}B$, or in an iterative way by the SIMPLE method with the FVM. In this respect, we compared the sensitivities found by both FEM and FVM. The FVM is implemented in the open-source CFD package OpenFOAM and FEM is implemented in Matlab with isoparametric polygonal elements.

2. RESEARCH METHOD

The flow over a backward-facing step with 1:2 sudden expansion is considered. Details of the geometry and mesh are shown in Fig. 1.

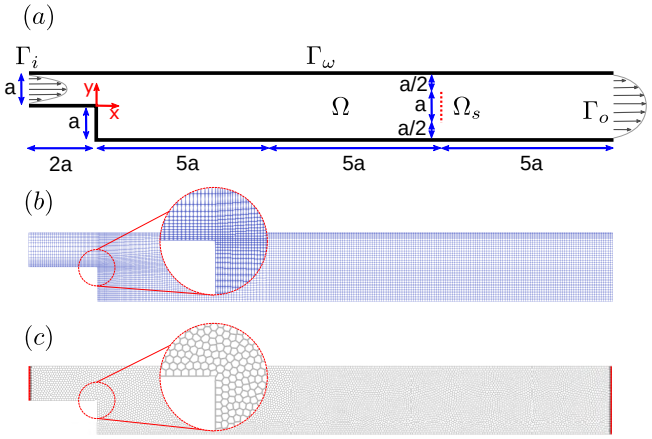

Figure 1. **Backward-facing step domain. (a) Geometry dimensions and boundaries, with $a = 0.02m$. (b) Structured mesh for FVM. (c) Polygonal mesh for FEM.**

In the inlet, the fully developed parabolic velocity profile for laminar flow is considered as:

$$U(y) = U_{max}\left[1 - \left(\frac{y}{a/2}\right)^2\right], \tag{1}$$

where a is the internal spacing in the inlet, and U_{max} is the maximum velocity.

Let Ω denote the flow domain, which is sketched in Fig. 1, and let Γ denote its boundary. The inflow and outflow part of the boundaries are denoted by Γ_i and Γ_o, respectively, and Γ_ω is the wall boundary. The system of governing equations in steady state form are given by:

$$-\nabla \cdot (2\nu \mathrm{D}(\boldsymbol{u})) + (\boldsymbol{u} \cdot \nabla)\boldsymbol{u} + \frac{\nabla p}{\rho} - \boldsymbol{f}_{\Omega_a} = 0, \tag{2}$$

$$\nabla \cdot \boldsymbol{u} = 0, \tag{3}$$

where $\boldsymbol{u}$ and p stand for velocity and pressure, respectively. $\boldsymbol{f}_{\Omega_a}$ stands for sources defined in the sub domain Ω_a, which could be dependent function of $\boldsymbol{u}$, $\nu = \mu/\rho$ is the kinematic viscosity, μ is the dynamic viscosity (sometimes also called the absolute viscosity), ρ is the density, and the rate of strain tensor is denoted by $\mathrm{D}(\boldsymbol{u}) = 1/2(\nabla \boldsymbol{u} + \nabla^{\mathsf{T}} \boldsymbol{u})$. For the case of Fig. 1, we utilise the following set of boundary conditions:

$$\boldsymbol{u}|_{\Gamma_i} = U(y), \qquad \boldsymbol{n} \cdot \nabla p|_{\Gamma_i} = 0, \tag{4}$$

$$\boldsymbol{u}|_{\Gamma_\omega} = 0, \qquad \boldsymbol{n} \cdot \nabla p|_{\Gamma_\omega} = 0, \tag{5}$$

$$\nu(\nabla \boldsymbol{u}) \cdot \boldsymbol{n} - \frac{1}{\rho} p\, \boldsymbol{n}|_{\Gamma_o} = 0, \tag{6}$$

where $\boldsymbol{n}$ is the outward unit normal.

2.1 CFD-Based Continuous adjoint method

Let's assume that the objective functional is defined as $\mathcal{J} = \mathcal{J}(\boldsymbol{u}, p, \varrho)$, and the system of governing equations by $\mathbf{R}(\boldsymbol{u}, p, \varrho) = 0$, where ϱ represents the design variable. The adjoint equations are derived by introducing a Lagrange function $\mathcal{L}$, reformulating the cost function as:

$$\mathcal{L}(\boldsymbol{u}, p, \varrho, \boldsymbol{v}, q) = \mathcal{J}(\boldsymbol{u}, p, \varrho) - \int_\Omega (\boldsymbol{v}, q)^{\mathsf{T}} \boldsymbol{R}(\boldsymbol{u}, p, \varrho)\, \mathrm{d}\Omega, \tag{7}$$

where $\boldsymbol{v}$ and q are Lagrange multipliers that are used to enforce the residuals $\boldsymbol{R}$ (the constraints equations). Through the introduction of Lagrange multipliers, the constrained optimization problem is converted into an unconstrained problem. After elaborating further using integration by parts (see Othmer (2008) for details), we obtain the system of adjoint equations:

$$-\nabla\cdot(2\nu\mathrm{D}(\boldsymbol{v}))-\nabla\boldsymbol{v}\cdot\boldsymbol{u}-(\boldsymbol{u}\cdot\nabla)\boldsymbol{v}+\frac{\nabla q}{\rho}-\frac{\partial\boldsymbol{f}_{\Omega_a}}{\partial\boldsymbol{u}}\boldsymbol{v}=\frac{\partial\mathcal{J}_\Omega}{\partial\boldsymbol{u}}\Big|_{\Omega_s}, \tag{8}$$

$$(-\nabla\cdot\boldsymbol{v})=\frac{\partial\mathcal{J}_\Omega}{\partial p}\Big|_{\Omega_s}, \tag{9}$$

with the adjoint boundary conditions:

$$\boldsymbol{v}_t|_{\Gamma_i-\Gamma_\omega}=0, \tag{10}$$

$$\boldsymbol{v}_{\boldsymbol{n}}|_{\Gamma_i-\Gamma_\omega}=\frac{\partial\mathcal{J}_\Gamma}{\partial p}\Big|_{\Gamma_s}, \tag{11}$$

$$\boldsymbol{n}\cdot\nabla q|_{\Gamma_i-\Gamma_\omega}=0, \tag{12}$$

$$\nu(\boldsymbol{n}\cdot\nabla)\boldsymbol{v}+\boldsymbol{v}(\boldsymbol{u}\cdot\boldsymbol{n})+\boldsymbol{n}(\boldsymbol{v}\cdot\boldsymbol{u})-\frac{q\boldsymbol{n}}{\rho}\Big|_{\Gamma_o}=\frac{\partial\mathcal{J}_\Gamma}{\partial\boldsymbol{u}}\Big|_{\Gamma_s}, \tag{13}$$

Once we know the $(\boldsymbol{v},q)$ values, we can determine the sensitivities with the optimality condition which states, that the adjoints $(\boldsymbol{v},q)$ reach their optimal values, when the Lagrange functional gradient is zero.

$$\delta_\varrho\mathcal{L}=\delta_\varrho\mathcal{J}-\int_\Omega(\boldsymbol{v},q)^{\mathsf{T}}\,\delta_\varrho\boldsymbol{R}\,\mathrm{d}\Omega. \tag{14}$$

2.2 The Brinkman penalization approach

In the Brinkman penalization approach (Khadra *et al.*, 2000) the momentum equation is penalized by a source term (Darcy term) i.e. a friction force proportional to the fluid velocity, in order to account for the presence of immersed solid regions in the fluid flow domain.

$$\boldsymbol{f}_{\Omega_a}=-\alpha\boldsymbol{u}, \tag{15}$$

where α is the inverse of the local permeability, which allows to differentiate low or high permeability areas. In the fluid region, α is equal to zero, and it signifies that no artificial friction force is added. In the solid region, α is equal to the relatively large value of the order $O(10^5)$ to set the velocity to near zero.

2.3 The Objective Function

We employee the functional of error:

$$\mathcal{J}_1=\frac{1}{2}\int_\Omega(\boldsymbol{u}-\boldsymbol{u}_{ref})^2\,\mathrm{d}\Omega, \tag{16}$$

where $\boldsymbol{u}_{ref}$ is a reference velocity. The power dissipation of the fluid device is also considered:

$$\mathcal{J}_2=-\int_\Gamma\Big(p+\frac{1}{2}|\boldsymbol{u}|^2\Big)\boldsymbol{u}\cdot\boldsymbol{n}\,\mathrm{d}\Gamma. \tag{17}$$

where $\boldsymbol{n}$ is the unit vector normal to the boundary Γ. Then, we compute the required derivatives needed by the adjoint system, as:

$$\frac{\partial\mathcal{J}_{1\Omega}}{\partial\boldsymbol{u}}=(\boldsymbol{u}-\boldsymbol{u}_{ref}), \tag{18}$$

$$\frac{\partial\mathcal{J}_{2\Gamma}}{\partial\boldsymbol{u}}=-\Big[\Big(p+\frac{1}{2}|\boldsymbol{u}|^2\Big)\boldsymbol{n}-(\boldsymbol{u}\cdot\boldsymbol{n})\boldsymbol{u}\Big], \tag{19}$$

$$\frac{\partial\mathcal{J}_{2\Gamma}}{\partial p}=-\boldsymbol{u}\cdot\boldsymbol{n}. \tag{20}$$

3. PARAMETRIC OPTIMIZATION

In order to meet the optimal design of sources, we need to use parameterized functions that allow us to manipulate its characteristic features. In this work, we use the following unitary magnitude functions:

- The **delta function** is used to represent point sources. We express this function as follows:

$$f_p(\boldsymbol{x}_o) = \delta(\boldsymbol{x} - \boldsymbol{x}_o). \tag{21}$$

  where the coordinate position $\boldsymbol{x}_o$ is a parameter that can be manipulated for design optimization. Notice that successive points form **line** sources.

  In general, both finite element and finite volume solvers provide information only at the nodal and center of elements, respectively. Discrete point sources in the model which don't coincide with the grid need to be interpolated to arbitrary points in the domain. In this work we adopt two interpolation approaches using shape functions, called, iterative inverse mapping and the Moving Least Square, for FEM and FVM respectively.

- The **exponential function** as expressed in Eq. (22) allow us to represent square area sources.

$$f_a = \left(\frac{1}{1+e^{-2k[(x-x_o)+r_x]}} - \frac{1}{1+e^{-2k[(x-x_o)-r_x]}}\right) \times \left(\frac{1}{1+e^{-2k[(y-y_o)+r_y]}} - \frac{1}{1+e^{-2k[(y-y_o)-r_y]}}\right), \tag{22}$$

  where x_o, y_o and r_x, r_y are center position and radius, in the x and y coordinate directions, respectively. k is a positive constant related to the sharpness of the function f_a.

3.1 Source Sensitivity

We aim to optimize the design of the source $\boldsymbol{f}_{\Omega_a}$ from Eq. (2). For that purpose, in the momentum equation, the source $\boldsymbol{f}_{\Omega_a}$ is the friction force kind, by adopting the Brinkman penalization approach as stated in subsection 2.2

Let's recall the optimality condition Eq. (14), from which we compute the sensitivity of the functional $\mathcal{J}$ with respect to changes of the design parameter ϱ.Then, the sensitivity regarding the design parameter ϱ results:

$$\frac{\mathcal{D}\mathcal{J}}{\mathcal{D}\varrho} = \delta_\varrho \mathcal{J} + \int_{\Omega_a} \boldsymbol{v} \cdot \delta_\varrho(\alpha \boldsymbol{u})\, \mathrm{d}\Omega. \tag{23}$$

4. NUMERICAL METHOD

Simulations were performed on a PC with the following specifications: CPU Intel Core3 M 370 2.40GHz, RAM DDR3 2.8GB 1066MHz. The FEM implementation was running in Matlab R2019b, adopting polygonal grids and the FVM was implemented in OpenFOAM. For the OpenFOAM implementation, the adjointOptimisationFoam implementation was adapted to obtain the adjoint variables.

5. RESULTS

The sensitivity of the design variable ϱ, is intimately related to the adjoint values as presented in previous section. In order to investigate the validity of these sensitivities, a comparison was made with the sensitivities evaluated by the FDM.

First, we consider the sensitivity of sources, for both their magnitude and position. We begin by showing the problem layout in 1D domain $\Omega(x) = (0, L) \in \mathbb{R}$ of length $L = 1\text{m}$. The primal equation is the second-order linear ordinary differential equation:

$$u\frac{\partial \phi}{\partial x} - D\frac{\partial^2 \phi}{\partial x^2} - f_{\Omega_a} = 0 \quad \text{in} \quad \Omega, \tag{24}$$

with Dirichlet and Neumann boundary conditions respectively:

$$\phi|_{\Gamma_i} = g_D \quad \text{and} \quad n_x D\frac{\partial \phi}{\partial x}\bigg|_{\Gamma_o} = 0. \tag{25}$$

The objective function and derivatives in this case have the form:

$$\mathcal{J}_3 = \frac{1}{2}\int_{\Omega_s} (\phi - \phi_{\Omega_r})^2\, \mathrm{d}x, \quad \frac{\partial \mathcal{J}_{3\Gamma}}{\partial \phi} = 0 \quad \text{and} \quad \frac{\partial \mathcal{J}_{3\Omega_s}}{\partial \phi} = (\phi - \phi_{\Omega_r}), \tag{26}$$

where ϕ_{Ω_r} is an scalar field computed with reference parameters values which define f_{Ω_a} and g_D is an specified value for the Dirichlet boundary condition. In each case we consider $u = 0.01m/s$ and $D = 0.005m^2/s$.

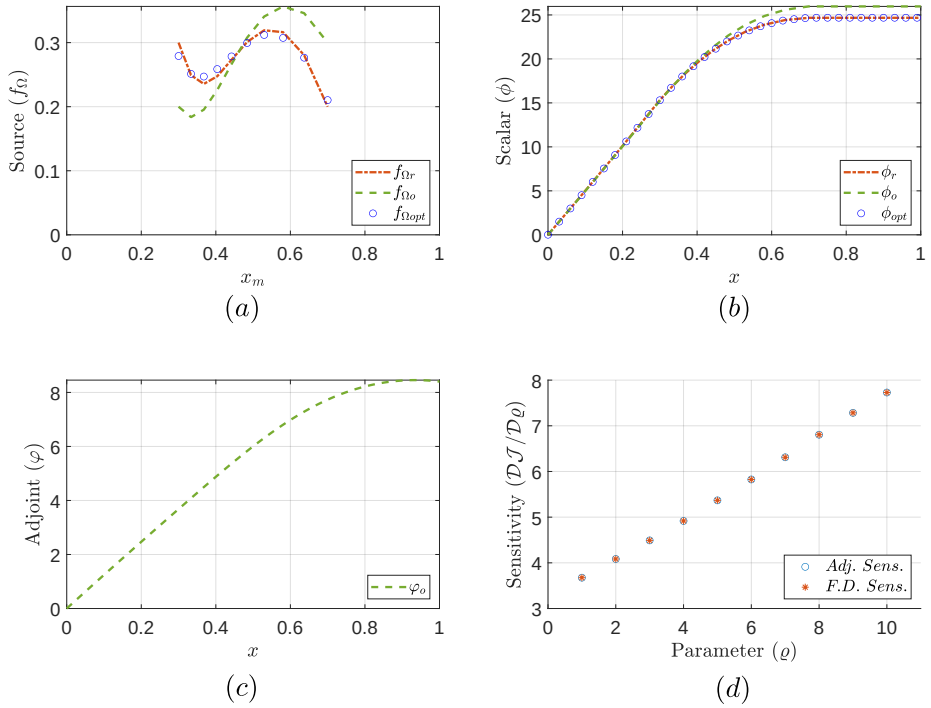

Figure 2. **Distributed source magnitude optimization for 1D case (a) source, (b) scalar and (c) adjoint profiles. (d) Sensitivity of each source.**

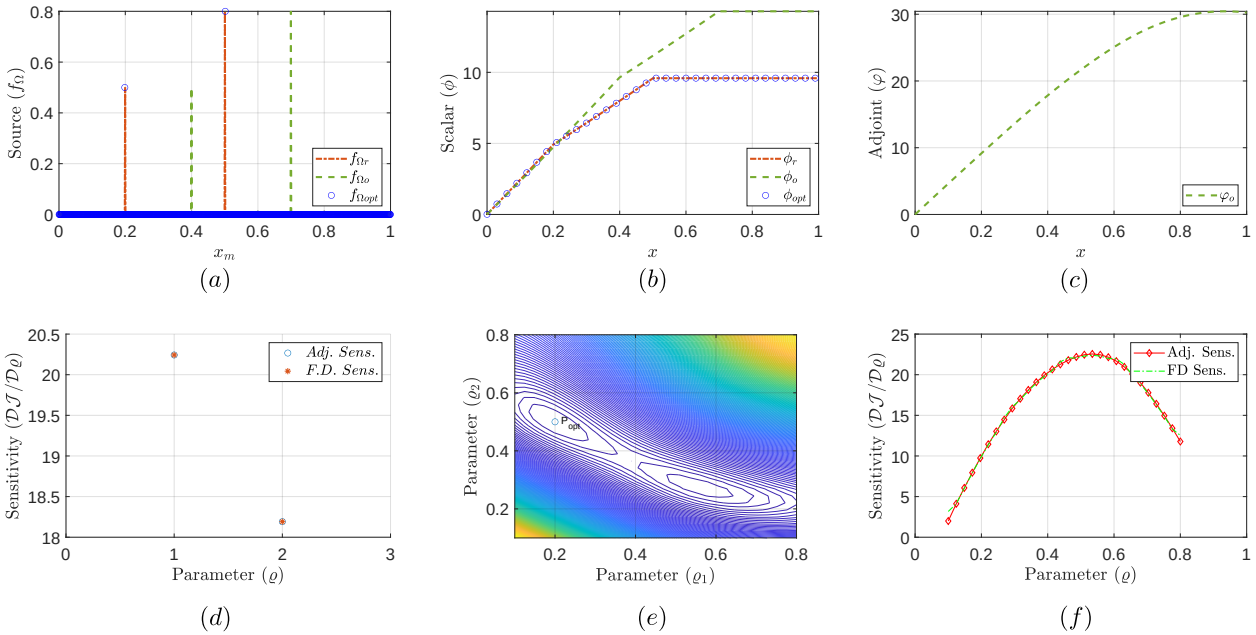

Figure 3. **Two point source position optimization for 1D case (a) source, (b) scalar and (c) adjoint profiles. (d) Sensitivity of each source at initial state. (e) Contour of objective function relative to the two parameters. (f) Sensitivity for a range of values of parameter 1.**

For 1D cases we consider the "inverse design optimization", that is, starting from the initial state variable ϕ_o obtained from f_{Ω_o} and approaching as closely as possible to the reference state variable ϕ_{Ω_r} obtained from an established f_{Ω_r}. The end result will be the optimized state variable ϕ_{opt} corresponding to $f_{\Omega_{opt}}$.

Figure 2 shows the case of a non-uniform distributed source. The sensitivity of the cost function ($\mathcal{J}_3$) relative to the magnitude of each source is proportional to the value of the adjoint at each position, as shown in Fig. 2d.

In Fig. 2a we notice that f_{Ω_r} and $f_{\Omega_{opt}}$ do not coincide completely, this is because we may have found a local minimum or the established tolerance is not small enough. Although, there is a significant difference between f_{Ω_o} and

f_{Ω_r}, the difference between the scalar fields ϕ_o and ϕ_r is relatively small.

Figure 3 shows the case of two point sources and its position optimization. Looking at Figure 3d and Fig. 3f, we confirm that the sensitivity of $\mathcal{J}_3$ in relation to the position of each one of sources is proportional to the value of the adjoint gradient computed at the position of each source. In Fig. 3 we can see that there are two minimum of the objective function relative to the position of sources. The minimum corresponding to f_{Ω_r} is indicated in the Fig. 3e with the symbol P_{opt}. Since we are using the gradient method, it will depend on the choice of our initial state condition to fall into any of the minimum. Given this, it is advisable to get a good knowledge of the physical phenomenon to set up the objective function and the initial parameters values.

Figure 4 shows the case of two area sources, of different sizes. Here the sensitivity of the objective function relative to the central position of each source is proportional to the integral of the adjoint spanning the entire size of each source. Then, the case is similar to that of the point sources of the previous case.

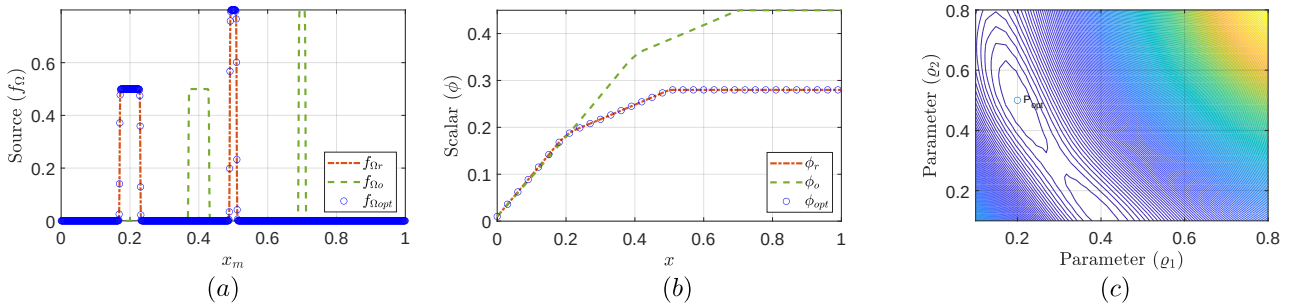

Figure 4. **Two area source position optimization for 1D case (a) source and (b) scalar profiles. (c) Contour plot of objective function relative to the two parameters.**

Figure 5 and Fig. 6 show the cases where f_{Ω_a} is dependent on ϕ, for the optimization of magnitude and position of area sources, respectively. In both cases the sensitivities calculated by the adjoint method and finite difference are practically the same, however when using the Quasi-Newton BFGS optimization algorithm, we are not able to reach the minimum, as f_{Ω_r} and $f_{\Omega_{opt}}$ are so far, as shown in Fig. 5a and Fig. 6a. Figure 5e and Fig. 6e show the contour plot of the objective function relative to the magnitude and position of sources, respectively, we notice that the global minimum P_{opt} is in a very flat zone, consequently, the algorithm by the gradient method fails or have difficulties to reach the global minimum.

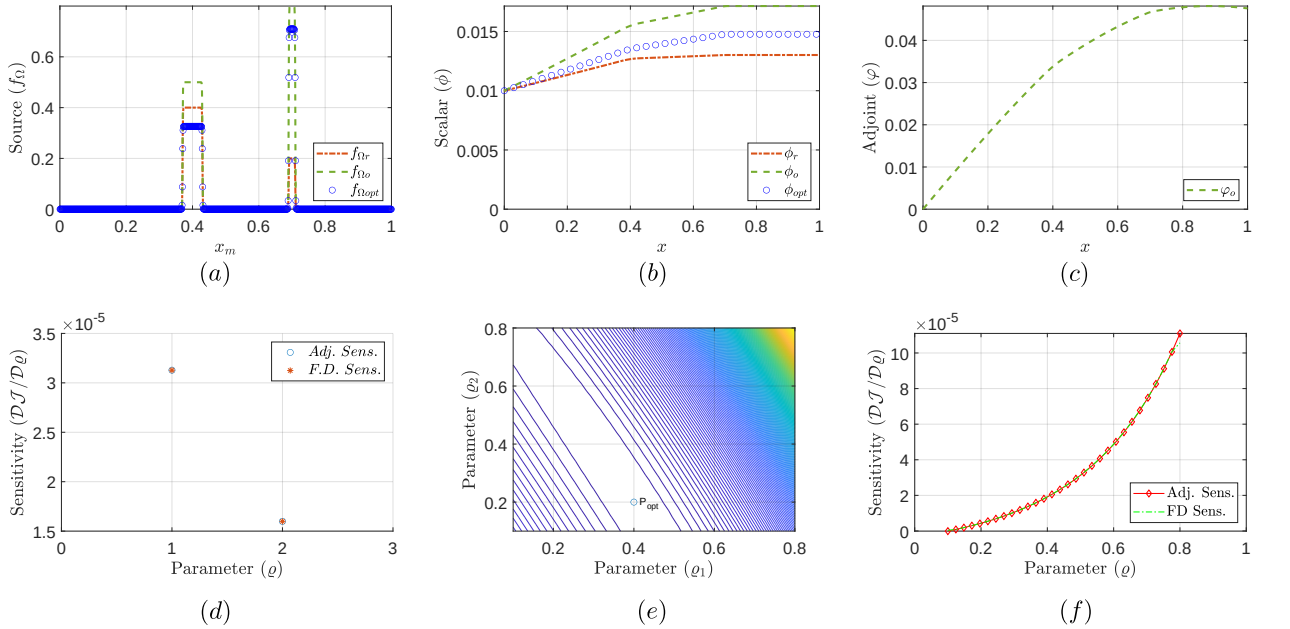

Figure 5. **Two area source magnitude optimization for 1D case (a) source, (b) scalar and (c) adjoint profiles. (d) Sensitivity of each source at initial state. (e) Contour plot of objective function relative to the two parameters. (f) Sensitivity for a range of values of parameter 1.**

For 2D case, flow over a backward-facing step is considered, as shown in Fig. 7. Two rectangular solid blocks are represented as sources using the Brinkman penalization approach. The initial coordinates and sizes of sources are presented in Table 1.

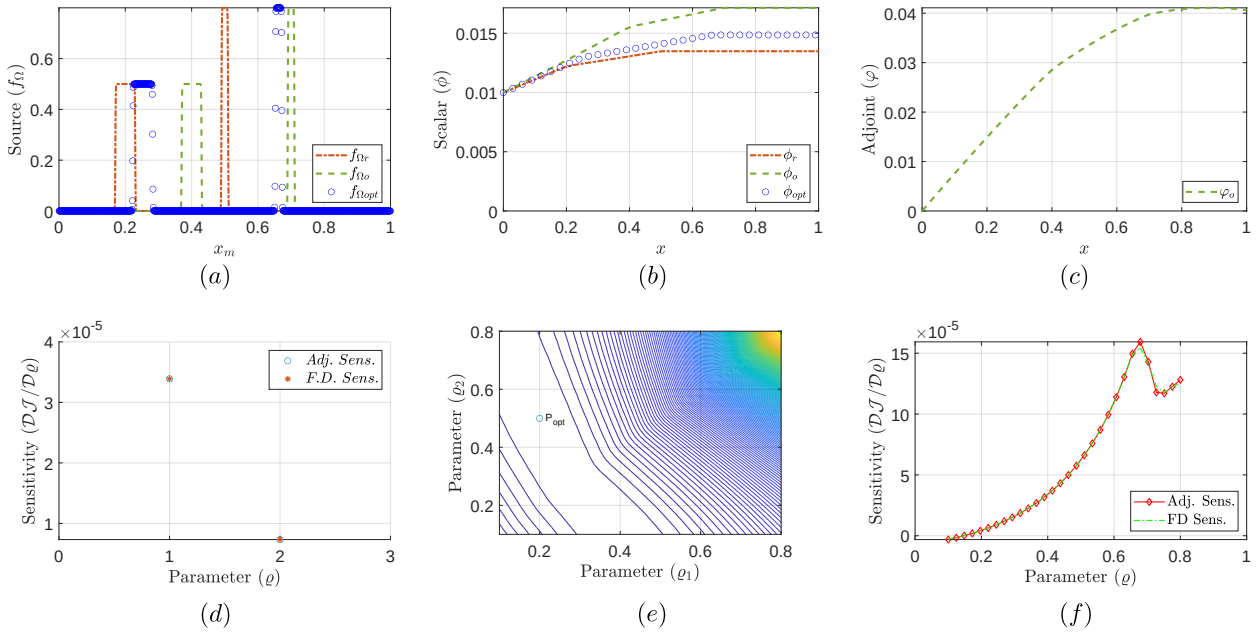

Figure 6. **Two area scalar dependent source position optimization for 1D case (a) source, (b) scalar and (c) adjoint profiles. (d) Sensitivity of each source at initial state. (e) Contour plot of objective function relative to the two parameters. (f) Sensitivity for a range of values of parameter 1.**

Table 1. **Initial coordinates and sizes of sources.**

Coordinates (m)		Sizes (m)	
x_{a1}	0.08	Rx_{a1}	0.01
x_{a2}	0.12	Rx_{a2}	0.002
y_{a1}	0.005	Ry_{a1}	0.002
y_{a2}	-0.005	Ry_{a2}	0.005

The sensitivity was calculated for the error objective function and total pressure loss, as can be seen in Figure 7e and Fig. 7f. The error objective function is a line of 20 points distributed in $y = 0.2$ and $-0.01 \leq x \leq 0.01$, in analogy to a sensor within the computational domain. We can see that there is a good agreement between the sensitivities.

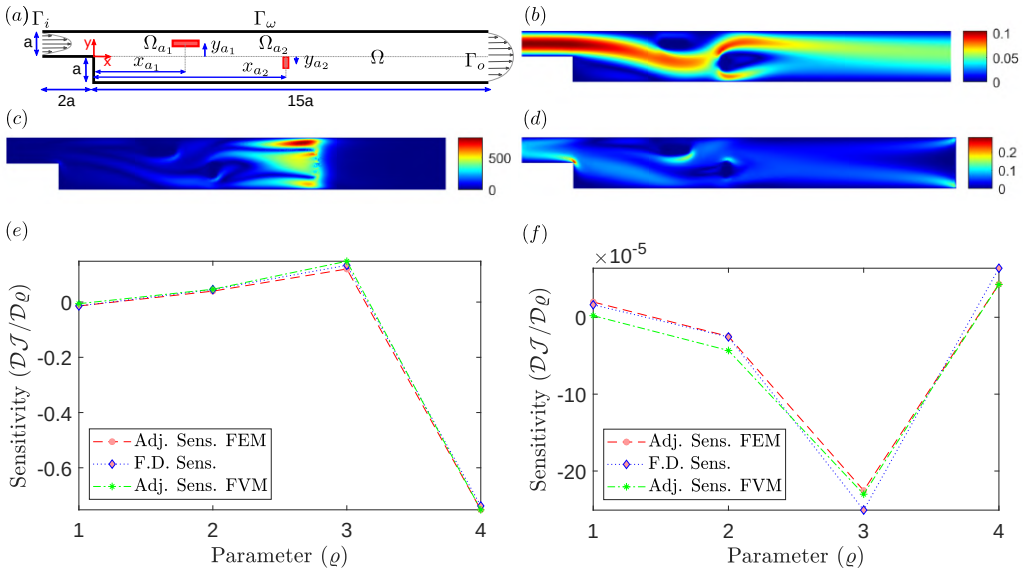

Figure 7. **(a) Sketch of geometry and dimensions for two area source controls. Results using FEM: (b) primal velocity field; (c) adjoint velocity field and (e) sensitivities for line error functional; (d) adjoint velocity field and (f) sensitivities for total pressure loss functional.**

Source position optimization is done with the Steepest Descent Method as follows:

$$\boldsymbol{x}_a = min(max(\boldsymbol{x}_a + \lambda \cdot \nabla \mathcal{J}, \boldsymbol{x}_{min}), \boldsymbol{x}_{max}). \tag{27}$$

Let us first consider the optimization of the position of the two area sources in Fig. 7. The limits that restrict the position of the sources are, $\boldsymbol{x}_{min} = (0.10, -0.01)$ and $\boldsymbol{x}_{max} = (0.12, 0.01)$, with a step of $\lambda = 10^{-4}$. Figure 8a and Fig. 8b show the velocity and pressure fields, for the final position of the source that minimizes the total pressure loss. Figure 8c shows that the objective function reaches its minimum in approximately 40 cycles.

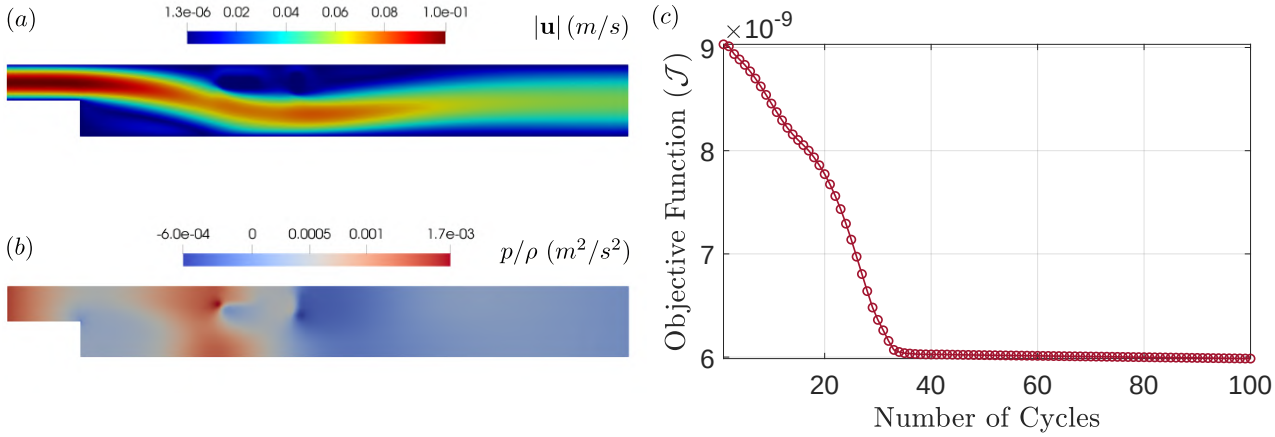

Figure 8. **Two area source position optimization for total pressure loss functional minimization. (a) Velocity and (b) pressure fields. (c) Variation of the objective function with the number of design cycles.**

Figure 9a and Fig. 9b show the optimal velocity fields where the error objective function at specific region of the computational domain is used, whose characteristics are detailed in Table 2.

Table 2. **Characteristics of line error objective function.**

	Case 1	Case 2
$x(m)$	0.2	0.15
$y(m)$	[-0.01,0.01]	[-0.015,-0.005]
No points	20	10
$\boldsymbol{u}_{ref}$	0.05	0.1

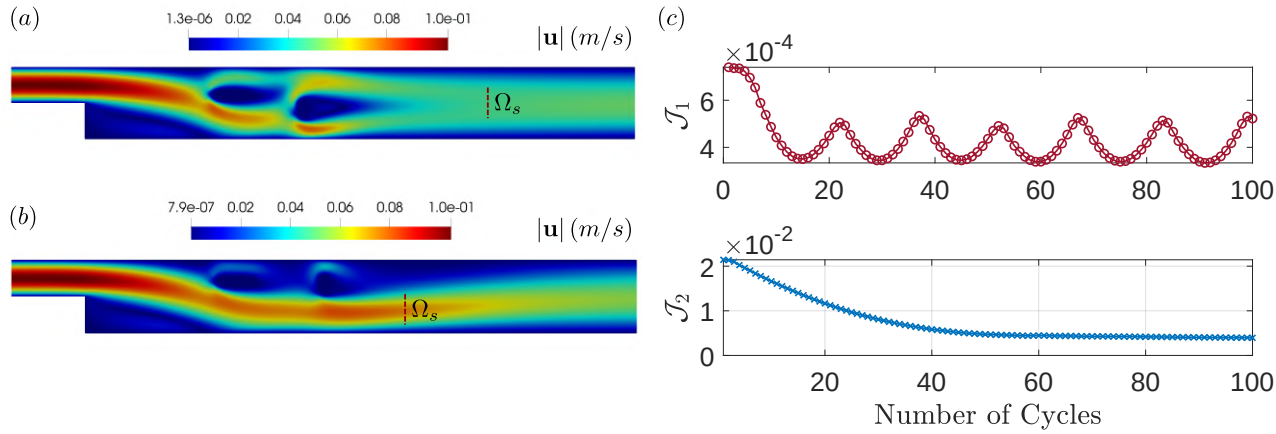

Figure 9. **Two area source position optimization for error functional minimization. Velocity fields for cases (a) 1 and (b) 2. (c) Variation of the objective function with the number of design cycles for both cases.**

These cases serve to exemplify how important it is to know the physical phenomenon of the problem and thus be able to formulate objective functions that can be fulfilled. For example, in both cases it is intended that the velocity be uniform equal to 0.05 and 0.1 in the x direction, respectively, however, this is not physically possible due to the deceleration of the fluid near the walls and the acceleration in the central part of the duct. Thus the final result will result in an average of the specified velocity $\boldsymbol{u}_{ref}$.

The variation of the objective function in Fig. 9c shows us that in the first case there is no convergence towards a single minimum, but rather there is an up and down variation, contrary to the second case where we can observe a convergence. The initial and final profile for both cases shown in Figure 10a and Fig. 10b indicates that in the first case the velocity profile does not have a significant change, unlike the second case where the fluid accelerates at the location of the sensor. This happens because the sensitivity is greater in the second case in relation to the first one.

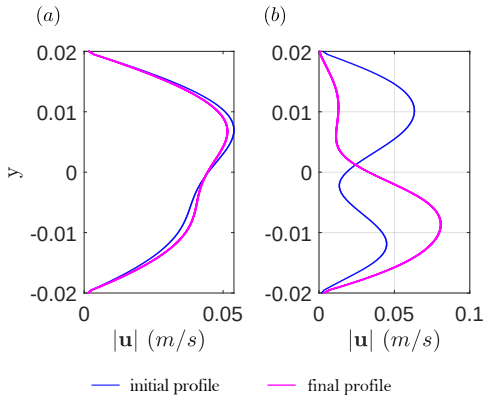

Figure 10. **Two area source position optimization for error functional minimization. Initial and final velocity profiles for cases (a) 1 and (b) 2.**

Practical application of source position optimization could be in valve design, in which we want to design the shape of the inner wall boundary. Figure 11 shows the results in different design cycles of the velocity field, pressure field and the function of interpolation shown in corresponding to sensitivities in the y directions respectively.

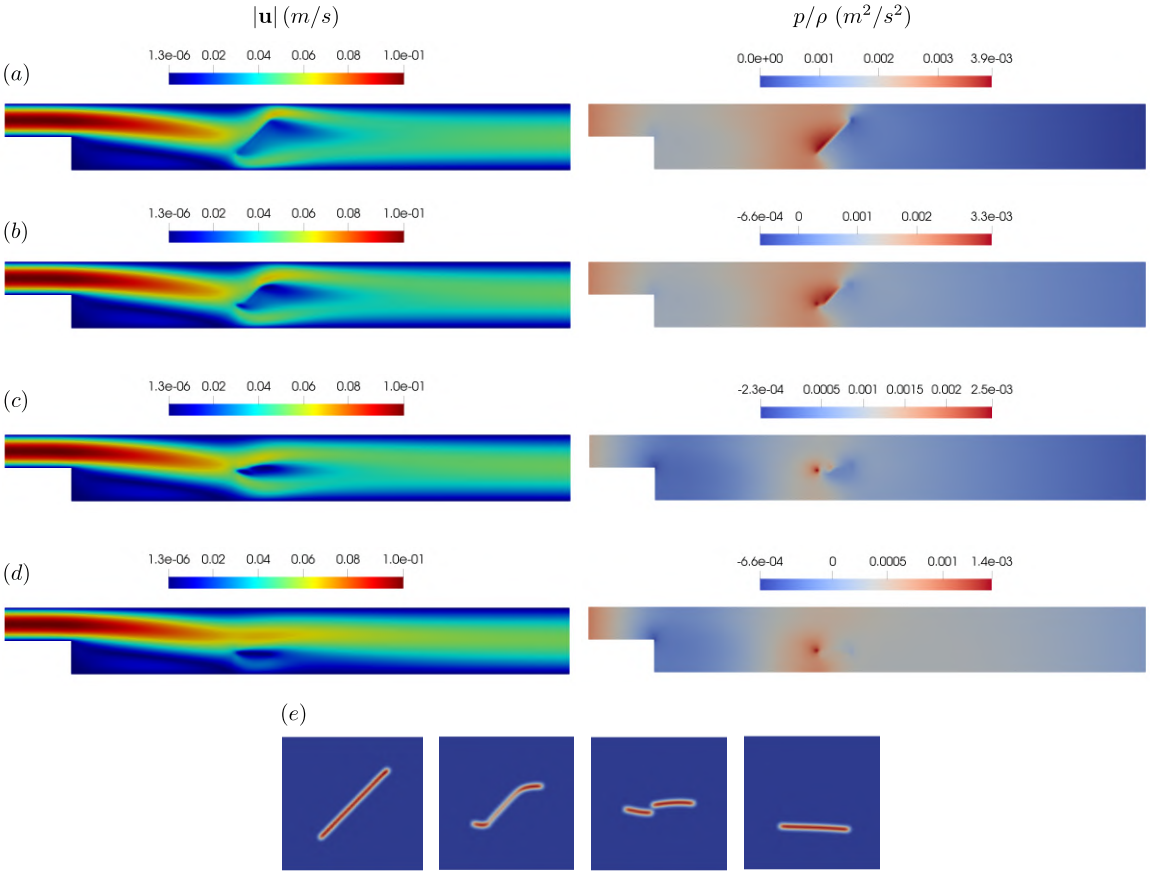

Figure 11. **Line source position optimization for total pressure loss functional minimization with movement in the y direction. Velocity and pressure fields for (a) initial, (b) 50, (c) 100 and (d) 200 number of design cycles. (e) Shape field of the interpolation function.**

Although the separation between points is not desirable, too much approximation between points is not either, since it generates distortion in the velocity and pressure field.

6. CONCLUSIONS

The optimal location and magnitude of discrete sources in the domain were studied. We presented the derivation of the sensitivities with respect to the coordinates and magnitude of the sources, using the continuous adjoint method. The sensitivities were compared with the sensitivities calculated by the Finite Difference Method (FDM), obtaining good agreement in all cases. The method was first presented in one dimension for a standard scalar transport in steady-state, followed by an extension to two dimensions.

It is necessary to formulate a restriction that allows us to represent an internal impermeable wall, paying attention to the adequate spacing between the source points and implement a most robust optimizer i.e. the Method of Moving Asymptotes (MMA).

7. ACKNOWLEDGEMENTS

We are grateful for the financial support provided by CNPq, the Brazilian Research Council.

8. REFERENCES

Boffi, D., Gastaldi, L. and Heltai, L., 2005. "The finite element immersed boundary method: model, stability, and numerical results". *Computational Methods for Coupled Problems in Science and Engineering*, , No. January 2014, pp. 56–69.

Eriksson, C., 2017. *Thermal design optimization by geometric parameterization of heat sources parameterization of heat sources*. Ph.D. thesis.

Khadra, K., Angot, P., Parneix, S. and Caltagirone, J.P., 2000. "Fictitious domain approach for numerical modelling of Navier-Stokes equations". *International Journal for Numerical Methods in Fluids*, Vol. 34, No. 8, pp. 651–684. ISSN 0271-2091. doi:10.1002/1097-0363(20001230)34:8<651::AID-FLD61>3.0.CO;2-D.

Kouhi, M., Houzeaux, G., Cucchietti, F. and Rodriguez, F., 2016. "Implementation of discrete adjoint method for parameter sensitivity analysis in chemically reacting flows". In *57th AIAA/ASCE/AHS/ASC Structures, Structural Dynamics, and Materials Conference, AIAA SciTech Forum*. pp. 1–19.

Liu, W., 2017. *Inverse Design of Inverse Design of Enclosed Environment by CFD-Based Adjoint Method*. Ph.D. thesis.

Nabi, S., Grover, P. and Caulfield, C., 2017. "Adjoint-based optimization of displacement ventilation flow". *Building and Environment*, Vol. 124, pp. 342–356. ISSN 03601323. doi:10.1016/j.buildenv.2017.07.030.

Othmer, C., 2008. "A continuous adjoint formulation for the computation of topological and surface sensitivities of ducted flows". *International Journal for Numerical Methods in Fluids*, Vol. 58, No. 8, pp. 861–877. ISSN 02712091. doi:10.1002/fld.1770.

Rimer, S.P., 2016. *Controlling Hazardous Releases While Protecting Passengers in Civil Infrastructure Systems*. Ph.D. thesis.

Soto, O., Löhner, R. and Yang, C., 2004. "An adjoint-based design methodology for CFD problems". *International Journal of Numerical Methods for Heat & Fluid Flow*, Vol. 14, No. 6, pp. 734–759. ISSN 0961-5539. doi: 10.1108/09615530410544292.

9. RESPONSIBILITY NOTICE

The author(s) is (are) solely responsible for the printed material included in this paper.